AN INVERSE FREE ELECTRON LASER ACCELERATOR EXPERIMENT

Iddo Wernick and T.C. Marshall
Department of Applied Physics, Columbia University, New York, NY 10027

CONF-9206193--18

DE93 003495

ABSTRACT

A free electron laser was configured as an autoaccelerator to test the principle of accelerating electrons by stimulated absorption of radiation (λ=1.65mm) by an electron beam (750kV) traversing an undulator. Radiation is produced in the first section of a constant period undulator (l_{w1}=1.43cm) and then absorbed (~40%) in a second undulator, having a tapered period (l_{w2}=1.8-2.25cm),which results in the acceleration of a subgroup (~9%) of electrons to ~1MeV.

The principle of using free electron laser [FEL] physics to accelerate electrons was described by Palmer [1] in 1972, however despite the extensive development of the FEL there has been no demonstration of the stimulated absorption of a laser pulse accompanied by acceleration of a group of electrons while the electron beam is traversing an undulator [IFEL]. The idea has been re-examined in more detail [2-4] and appears to offer some promise to achieve an acceleration gradient ~ 1MV/cm in linear accelerators. In the electron rest frame, the magnetostatic field of the undulator is transformed into an electromagnetic wave which beats with the laser; acceleration occurs by keeping the phase of the electrons constant with respect to the beat wave, by varying the undulator period and/or magnetic field as the particle energy increases. We have devised a relatively simple experiment, done on the Columbia FEL facility [5], which demonstrates that acceleration does occur.

The Columbia FEL operates at a wavelength of ~1.6mm and produces about five MW from a 750kV electron beam. As there is no powerful laser source at this wavelength, we have configured the experiment as an "autoaccelerator"[IFELA] in which a subgroup of electrons is accelerated by the "inverse FEL" mechanism at the expense of the average energy of the entire beam. This is done by separating the undulator into two sections.

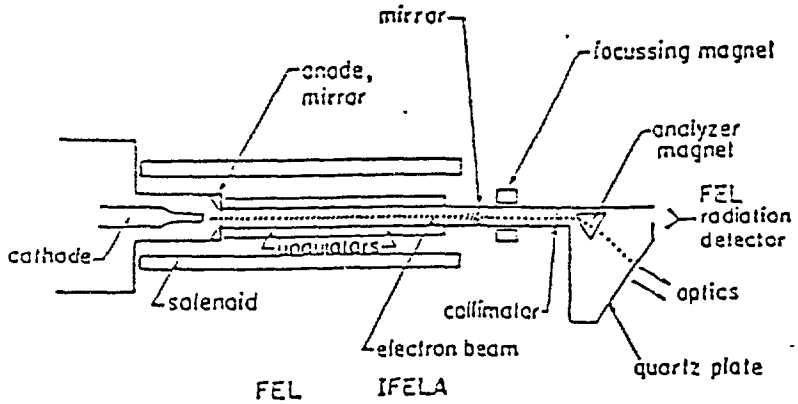

Figure 1: Schematic of the IFELA and the magnetic spectrometer. Electron emission occurs from a cold graphite cathode in a field-immersed diode, the beam is formed by a 4mm dia. aperture in a graphite anode, which also serves as the upstream mirror of the resonator.

Third Workshop on Advanced Accelerator Concepts
Port Jefferson, NY 14-20 June 1992
FG02-91ER 40669

The first section [Fig 1] together with a pair of 75% reflecting coaxial mirrors develops FEL radiation which grows from noise to saturated intensity and causes a bunching of the electrons. These particles then enter the second section of the undulator where the period is increased and then tapered along the axis so that a subgroup of electrons is accelerated as stimulated absorption of the wave occurs. We report measurements of this nonlinear absorption together with the electron energy spectrum. The accelerator section acts as a load for the oscillator, but its absorption is not high enough to prevent oscillation of the entire system.

Table I summarizes the parameters of the IFELA experiment. The undulator is a bifilar helical winding which provides a transverse field of order 600G following an adiabatic entry region.

Table I : Operating Conditions of the Columbia IFELA

Beam Energy	750-800kV
Beam Diameter	4mm
Beam current	150A
Pulse length	150nsec
Drift tube diameter	11mm
Undulator: first section	l_{w1}= 1.4cm
	B⊥= 600G
	length, 40cm
Undulator: second section	l_{w2}= 1.8-2.25cm
	taper= $\frac{1}{l_w}\frac{dl_w}{dz}$=0.0067cm^{-1}
	B⊥=400G
	length= 37.5cm

The beam is guided and focused along the drift tube by a uniform solenoidal field ~1T which causes "Group I" orbits [6]. The FEL power examined by a grating spectrometer shows a carrier wavelength of 1.6mm together with a pair of sidebands which carry about one-third of the total power; it was found that only the carrier was absorbed by the acceleration process [7]. The downstream mirror is polished graphite with a small hole on its axis followed by a collimator which forms the objective of the electron beam optics. A focusing solenoid guides the electrons beyond the fringe field of the solenoid. A dipole field using triangular polefaces deflects the beam and disperses the electrons onto a quartz viewing plate where the impact causes substantial Cerenkov light [8] (the quartz is painted with an opaque graphite film on the vacuum side). The light from the energetic electrons is directed to two lead-shielded photomultipliers located in a shielded room with the other electronics. The magnetic spectrometer is calibrated by using the electron beam with no undulator. The use of two photocells permits one photocell to monitor the principal group near the injection energy while the other scans the energy channels for the accelerated electrons.

The undulator in the IFELA section is designed using a numerical model to choose the appropriate field and taper. We use a set of equations [5] that models the electron motion in 1D along a single pass through the system and a self-consistent set of 2D field equations.

$$\frac{d\psi_i}{dz} = k_W + k_S - \frac{k_S}{\sqrt{1 - \frac{1+a_W{}^2 + 2a_W\, a_S \cos\psi_i}{\gamma_i{}^2}}} + \frac{\partial\Phi}{\partial z} \qquad (1)$$

$$\frac{d\gamma_i}{dz} = -\frac{a_W a_S k_S}{\gamma_i} \sin\psi_i + \frac{2\omega_p{}^2}{k_S c^2} [<\cos\psi>\sin\psi_i - <\sin\psi>\cos\psi_i] \qquad (2)$$

$$(\nabla_\perp{}^2 + 2ik_S \frac{\partial}{\partial z} + 2i \frac{\omega}{c^2}\frac{\partial}{\partial t}) u(r,t) = -F\frac{\omega_p{}^2 a_W}{c^2} < \frac{e^{-(\psi-\Phi)}}{\gamma} > \qquad (3)$$

Equation 1 is used to determine the phase Ψ of the electrons with respect to the signal wavefront as the electrons traverse the undulator. Equation 2 is the energy equation for the electrons and finally equation 3 is the 2D wave equation which describes the signal growth. The "Raman" term (i.e. terms $\propto \omega_p{}^2$) which accounts for the longitudinal space charge electric field from the electron bunches is included and is necessary to obtain the correct growth rate in the FEL section and the correct interaction in the IFELA section. The electron beam in the experiment has normalized parallel momentum spread ~ 1% [9], and is represented in the numerical study as a "cold" beam, since the trapping width, $\Delta\gamma/\gamma \propto \sqrt{a_S a_W}$ where a_S and a_W are the normalized vector potentials of the signal and undulator fields, is much larger than 1%.

The magnetic field of the FEL undulator section was chosen so that the power would grow roughly a factor of 25 in 40cm. This gain will sustain oscillation and results in a signal which reaches power saturation at the point where the electrons enter the IFELA section. The saturated power intensity on the beam axis, ~ 10MW/cm^2, is consistent with the power output from an FEL oscillator device very similar to this one [10]. It is found numerically that the wave amplitude is reduced by one-half as it reaches the end of the IFELA undulator as a subgroup of the trapped electrons is accelerated to ~1MV. The code includes no slippage and therefore does not account for sideband radiation; hence the measured absorption of the FEL power by the accelerator module will be less than the model predicts. The taper of the undulator which optimizes the absorption and acceleration is found through trial and error of the numerical study and corresponds to an acceleration gradient of ~7kV/cm in this test experiment. The taper is used to generate a variable-period helix which is mapped onto a section of phenolic tube and then cut to specification "by hand". Measurements of the actual undulator period taper and magnetic field taper are then incorporated into the code to simulate the actual experimental situation. Once the taper is chosen, a series of simulations show that the acceleration is not very sensitive to variation in FEL power or undulator field, however, increasing the power input to the IFELA section will accelerate more electrons. The field in the IFELA undulator can be varied independently of the FEL undulator; both are powered by a capacitor bank discharge synchronized to the accelerator timing system.

A set of representative data is shown in Fig 2. Shots are selected for a relatively flat diode voltage history, with electron energy near resonance. A determining signature as the electron beam energy reaches the design value is a

decrease of transmitted FEL power accompanied by an increase of light signal in the photomultipliers which respond to the accelerated electrons. The energy bins are separated by the resolution of the electron beam optics. Background light,obtained from operation of the apparatus with zero undulator field, is subtracted from the signal. The transmitted FEL power is monitored by a Schottky-barrier diode detector located

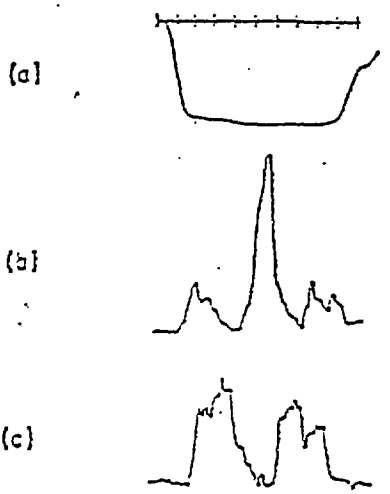

Figure 2. Representative signals obtained in the experiment. (a) Accelerator voltage, -800kV maximum; (b) signal from photocell monitoring 1MV electrons, showing a burst of electrons at middle of trace; (c) FEL power transmitted through the IFEL stage, showing absorption in middle of trace; 20nsec/div, horizontal scale.

along the beam axis. It is found that the fraction of power absorbed does not depend sensitively upon the power level itself. This behavior is to be expected from the model, which shows that increases in power absorbed result in more accelerated electrons but not necessarily higher electron energy.

Figure 3a displays results from a numerical simulation of the experiment showing the growth of the FEL signal, followed by the attenuation of the wave in the accelerator section. Fig 3b shows experimental data giving the FEL power transmitted through the accelerator section. This shows that there is a reduction of emitted power by ~40% in the vicinity of the resonant energy of the design. By reducing the undulator field in the accelerator section to 250G , the amount of observed absorption decreases to about 25% of the incident power. The study of the FEL spectrum [7] shows that the sidebands of the FEL power spectrum are not absorbed by the accelerator to a measurable amount, and therefore the reduction of the incident carrier intensity [~75%] indicated in the numerical simulation is larger than would be obtained if the sideband power is included in the measurement, as was the case.

Figure 4 shows the measured electron energy spectrum. The data is compared with the numerical simulation, run according to the experimental conditions. The computed spectrum is processed so that the ordinate corresponds to the number of simulation electrons contained in a bin having the same width as the experimental bin. The relative number of electrons accelerated and the acceleration energy are in good agreement with the numerical model. According to numerical simulation the smaller peak which occurs at $\gamma = 2.2$ does not result from the acceleration process.

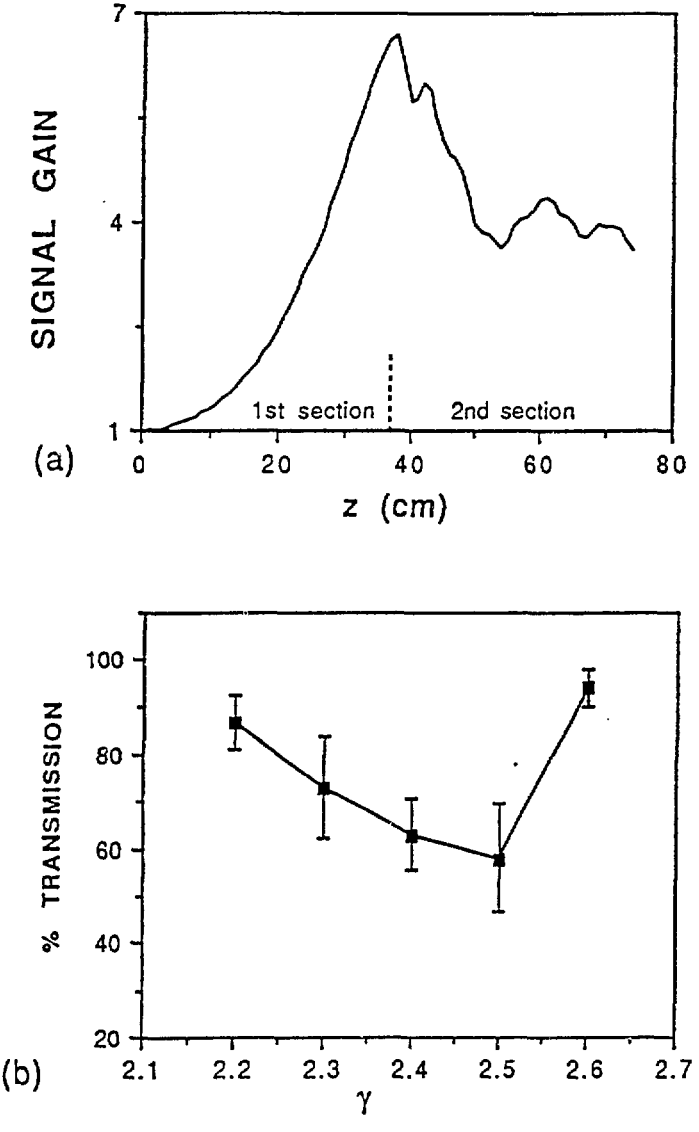

Figure 3. (a) Numerical result showing growth of FEL signal (initial intensity = 0.3MW/cm2) and attenuation in the IFELA section (begins at z = 37.5cm); (b) Radiation transmitted through the IFELA section as a function of initial electron beam energy. Parameters of simulation taken from Table I. Error bars indicate standard deviation of the data.

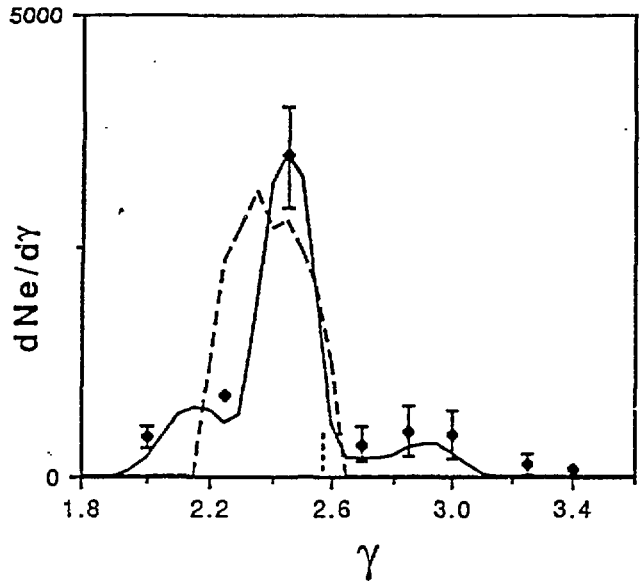

Figure 4. Measured electron energy spectrum(solid points);Electron energy spectrum obtained from simulation, at the exit from the IFELA(solid line); Electron energy spectrum obtained from simulation, at entry to the IFELA section(dashed line). The dotted vertical line denotes the injection energy.

For comparison, the dashed line on Fig 4 shows the electron spectrum computed (but not observed) at the end of the FEL section only; one notes there is a rapid cutoff of electrons having energy in excess of $\gamma = 2.7$, which is well below the energy of the accelerated group. Thus electrons at ~1MV have energy beyond the broadened distribution which results from the bunching and trapping of electrons from the FEL interaction. Electrons above the injection energy in FELs have been observed[11, 12] however they are not "accelerated" by the IFEL mechanism. The number of accelerated electrons is about 9% of the total number, as can be estimated from Fig 4. The ratio of the power required to accelerate these electrons to the overall power of the electron beam is about 3%, which is less than the efficiency of the FEL (4-6%).

In an actual IFEL where the radiation is supplied by an external laser, the undulator field can be considerably larger (roughly a factor of ten greater than in our experiment) and the intensity of the laser wave can be higher by perhaps a factor of a thousand. Taking a 10.6μ laser wavelength as an example our observed acceleration gradient ~ 7kV/cm would scale up by a factor of ~100 for such a device. Techniques exist to control synchrotron radiation losses which are no longer negligible at high energy [3]. Our success with the experiment and its interpretation suggests that the IFEL is a promising technology for an "advanced accelerator" demonstration.

ACKNOWLEDGMENT

This research is supported by the NSF, grant ECS -89-13066, DOE grant 02-91ER40669, and ONR grant N00014-89-J-1652. The assistance of Y-P Chou in the early stages of this project is greatly appreciated.

REFERENCES

1. R. B. Palmer, J. Appl. Phys. 43, 3014 (1972).
2. P. Sprangle and C. M. Tang, IEEE Nucl. Sci. NS-28, 3346 (1981).
3. E. D. Courant, C. Pellegrini, and W. Zakowicz, Phys. Rev. A32, 2813 (1985).
4. A. van Steenbergen and C. Pellegrini, private commun.
5. A. Bhattacharjee, S. Y. Cai, S. P. Chang, J. W. Dodd, A. Fruchtman, and T. C. Marshall, Phys. Rev. A40, 5081 (1989).
6. L. Friedland, Phys. Fluids 23, p.2376 (1980).
7. T. C. Marshall, A. Bhattacharjee, S. Y. Cai, Y. P. Chou, and I. Wernick, Nuclear Instruments and Methods in Physics Research A304, 683 (1991).
8. B. Kulke, M. J. Burns, and T. J. Orzechowski, LLNL Report UCRL-95598.
9. S. C. Chen and T. C. Marshall, IEEE J. Quantum Electronics QE-21, 924 (1985).
10. F. G. Yee, T. C. Marshall, and S. P. Schlesinger, IEEE Trans. on Plasma Science 16, 162 (1988).
11. A. H. Lumpkin and R. B. Feldman, Nucl. Instruments and Methods in Physics Research, A259, 19 (1987).
12. T. I. Smith, J. C. Frisch, R. Rohatgi, H. A. Schwettman, and R. L. Swent, Nucl. Instruments and Methods in Physics Research A296, 33 (1990).

DISCLAIMER